Journal homepage:http://revues.imist.ma/?journal=jasi

ISSN: 2550-4800

https://doi.org/10.48442/IMIST.PRSM/jasi-v11i1-3.31990

JASI JOURNAL OF APPLIED SURFACES AND INTERFACES

Fluorescent carbon quantum dots from Phoenix Dactylifera fruit pulp for UV radiation protection

F. O. Oyedeji [1], O. S. Bankole-Ojo [2,]*

[1] *Department of Chemistry, University of Ibadan, Ibadan, Oyo State, Nigeria.*
[2] *Department of Physical and Earth Sciences, Crawford University, Faith city, Igbesa, Ogun State, Nigeria.*

Received 18 April 2022; Revised 26 June 2022; Accepted 01 July 2022.

Abstract: *Carbon quantum dots (CQDs) have attracted significant attention due to their wide range of applications. These include biosensing, bioimaging, wound healing and antibacterial applications. In this study, we examine the potential Ultraviolet (UV) radiation protection role of CQDs towards the development of viable sunscreens. The CQDs will serve as a less toxic and bio-compatible alternative to the more toxic sunscreen actives used in commercial products. Phoenix dactylifera (date) fruit pulp was used as a promising precursor for the synthesis of fluorescent CQDs. The effects of reaction temperature and reaction time on the mass yield, hydrodynamic size and zeta potential were evaluated. The morphology and surface groups were studied before and after dialysis. The optical properties of the CQDs were examined spectrophotometrically, and the sun protection factor was calculated to obtain an insight into whether the CQDs are suitable for use as filters for the development of new sunscreens. From the results obtained, considerable sun protection factor values were obtained at small CQDs concentrations. This potentiates their use for the development of viable and less toxic sunscreens.*

Keywords: *Carbon quantum dots, Phoenix dactylifera, UV protection, Sunscreen, Sun Protection Factor.*

1. Introduction

Healthy exposure to sunlight has many health benefits, however, prolonged exposure to sunlight has been associated with sunburn, accelerated skin aging and skin cancer. Prolonged ultraviolet light exposure has been identified by the World Health Organization to be carcinogenic [1]. The UV-C (200-280 nm) is the most damaging type of ultraviolet irradiation with respect to the skin. It is filtered by the ozone layer and thus, bears no threat to the skin [2]. The UV-B (280-320 nm) is the most dangerous with energy exponentially higher than that of UV-A (320-420 nm) type. This implies that it bears erythemal power that is a thousand times greater than that of UV-A [3,4]. Sunscreens have been proven to protect the skin by reducing the impact of UV radiation. Several compounds have been synthesized and examined based on their ability to absorb UV radiation. These compounds are generally categorized into two main categories namely: organic UV absorbers and inorganic photoactive compounds [5].

The organic compounds are oftentimes less photostable and considerably toxic while the inorganic photo-actives have a tendency to agglomerate when used at higher concentrations. Therefore, there has been a strong demand for new biocompatible compounds that can be used as UV absorbers for sunscreens [6].

Carbon quantum dots (CQDs) have gained much attention in the scientific circles due to their chemical/thermal stability, biocompatibility, low toxicity, high water solubility, inexpensive cost and optical properties [7]. CQDs have being used in applications such as imaging, sensing, medical diagnosis, photovoltaics and photocatalysis. Additionally, CQDs have been found to exhibit other non-fluorescent properties, such as anticancer, antibacterial and wound healing properties [8-12].

CQDs are usually quasi-spherical with sizes below 10 nm. They are composed of amorphous to crystalline carbon base. Their framework is characteristically made up of sp2-graphitic carbon combined through the presence of sp3-hybridized carbon [13]

The physicochemical properties of CQDs can be easily controlled through surface functionalization and surface passivation. The solubility of CQDs can be modified based on the type of surface groups, which is controlled by the synthesis route and surface functionalization [14]. CQDs are particularly biocompatible with minimal or no toxicity and they are suitable for drug delivery, cosmetics, bio-imaging and bio-sensing applications, thus, these properties can be utilized to produce multifunctional sunscreens. Chatzimitakos et al. synthesized CQDs from the microalgae, *Dunaliella salina* and citric acid separately. They demonstrated that biogenic CQDs derived from *Dunaliella salina* exhibited an enhanced sun protection factor compared to CQDs from citric acid [15].

In this study, we synthesized CQDs from date (*Phoenix dactylifera*) fruit pulp. The morphological and surface properties of the biogenic CQDs produced under different reaction temperatures and reaction times. The

* *Corresponding author: E-mail: sciforch@hotmail.com (Olufunsho Samuel Bankole-Ojo)*

sun protection factor of the CQDs was determined at different concentrations using a UV/visible spectrophotometric method to evaluate their UV radiation protection potential for possible sunscreen applications.

2. Experimental

2.1. Collection and preparation of plant materials

The *Phoenix dactylifera* fruits were purchased between August and November from the Polimeraas: The Farmer's House, Nacharam - Mallapur Rd, MBD Complex, HMT Nagar, Tarnaka, Hyderabad, Telangana 500007, India, (17º42'29.9" N, 78º.54'61.6" E). Taxonomic identification was done by Dr. G. Baskar Rajan, the head of the botanical garden. Date fruits were washed with deionized water and cut open to remove the seeds. The date fruits were thinly sliced and stored at -20 °C in a freezer.

2.2. Synthesis of carbon quantum dots

Typically, 10 g of the thinly sliced date fruits was blended with 150 mL of deionized water and transferred into a round bottom flask placed in a silicone oil bath. The solution was refluxed under continuous stirring. The reaction was continued for 12 hours until the color of the solution turned dark brown. The solution was dialyzed against 1 liter of deionized water using dialysis membrane (MWCO of 1000 Da). During the dialysis process, the water was changed every two hours. The aqueous solution of carbon quantum dots was stored at -4 °C for further experimentation.

2.3. Mass yield determination

The aqueous solution of the carbon quantum dots was lyophilized at -80 °C under vacuum for 6 hours to obtain the solid product. % Mass yields were determined at varied temperatures and times. The % mass yield was calculated according *to the formula:*

$$\%Mass\ yiel = \frac{Mass\ of\ CQD*100}{Mass\ of\ initail\ pulp} \quad (1)$$

2.4. Characterization of CQDs

Transmission electron microscopic studies were performed using a JEOL JEM-100CX transmission electron microscope to examine the size and morphology of the CQDs. The hydrodynamic size and zeta potential of the CQDs were measured using Nanosizer Nano ZS, Malvern at an ambient temperature of 25 °C. Samples were prepared by further diluting the particle stock suspensions in appropriate solvents (1:200 w/v), with prior ultrasonication and filtration processes. Size measurements were performed in the non-invasive backscattering mode (NIBS) at a scattering angle of 173º using polystyrene disposable cuvettes. Fourier Transform Infrared (FTIR) spectroscopy study was performed using Thermo Nicolet Nexus 670 Fourier Transform Infrared spectrophotometer. The groups attached to the carbon quantum dots were investigated by FTIR spectroscopy using the KBr disc method at an ambient temperature of 25 °C. UV-vis absorption spectra were obtained using a Shimadzu 220V (E) UV-Visible spectrophotometer. Measurements were performed at an ambient temperature of 25 °C. Fluorescence spectroscopic studies were performed using a Horiba Fluoromax 4 spectrometer. Measurements were performed at an ambient temperature of 25 °C.

2.5. Sun Protection Factor (SPF) calculation

The SPF of the CQDs were determined by recording the UV spectrum between 290 and 320 nm. SPF values were obtained using the Mansur's Equation shown as equation (2) below, based on previous studies [16,17].

$$SPF = CF \times \sum EE(\lambda) \times I(\lambda) \times ABS(\lambda) \quad (2)$$

where CF is the correction factor (=10), EE(λ) is the erythemogenic effect of radiation at wavelength λ, I(λ) is the solar light intensity at wavelength λ and ABS(λ) is the absorbance of the tested solution at a wavelength λ. The EE(λ) × I(λ) values are constant.

3. Results and discussion

3.1. Percentage mass yield distribution

The variation of percentage mass yield values for carbon quantum dots obtained at different reaction temperatures and a fixed reaction time of 12 hours are presented in Fig.1a. Average percentage mass yields of 0.027, 1.152, 4.519, 4.543 and 4.555 % were obtained at reaction temperatures of 110, 140, 170, 200 and 230 °C, respectively. The mass yields of the carbon quantum dots increased between 110 and 170 °C. Little change was observed in the mass yield beyond 170 °C. This highlights the possibility of the carbon burst which produced the carbon dots occurring at temperatures around 170 °C. Carbon quantum dots synthesized at 170 °C were used for further applications in this study.

The variation of percentage mass yield values for carbon quantum dots obtained at different reaction times and a fixed reaction temperature of 170 °C are presented in Fig.1b. Average percentage mass yields of 3.131, 4.503, 4.519, 4.563 and 4.587 % were obtained at reaction times of 4, 8, 12, 16 and 20 hours, respectively. The mass yields of the carbon quantum dots increased strongly between 4 and 8 hours. Beyond 8 hours, the percentage mass yield of the CQDs increased slightly. Subsequent synthesis was performed for 12 hours. Reaction temperature had a more consequential effect than the reaction time on the %mass yield.

3.2. Dynamic Light Scattering (DLS) analysis

Fig.2 Shows the DLS results for CQDs at different (a) temperature (b) time. From the figure it can be seen that, at a fixed time of 12 hours, the average hydrodynamic sizes of CQDs synthesized at 230 °C and 200 °C were very

close 10.2 and 10.4 nm, respectively. Average hydrodynamic sizes increased to 14.3 nm at a reaction temperature of 170 °C. CQDs synthesized at 140 and 110 °C had average hydrodynamic sizes of 25.4 and 70.1 nm, respectively. At a fixed temperature of 170 °C, the average hydrodynamic sizes of CQDs at different reaction times were determined. CQDs synthesized for 20 hours and 16 hours had close average hydrodynamic sizes of 9.6 and 9.9 nm. Average hydrodynamic sizes increased to 14.3 nm at a reaction time of 12 hours. CQDs synthesized for 8 hours and 4 hours had average hydrodynamic sizes of 37.3 and 49.5 nm, respectively.

3.3. Zeta potential measurements

Zeta potentials of the synthesized CQDs were determined to obtain the surface charge (Fig.3). This technique gives insight on the CQDs surface attributes with respect to attached hydrophilic groups like hydroxyl, carbonyl and carboxyl groups. The zeta potential generally decreased with increasing reaction temperatures and reaction times. Increase in temperature from 110 to 170 °C resulted in a significant reduction in zeta potential values. The increase in reaction time translated to less significant decrease in zeta potential values.

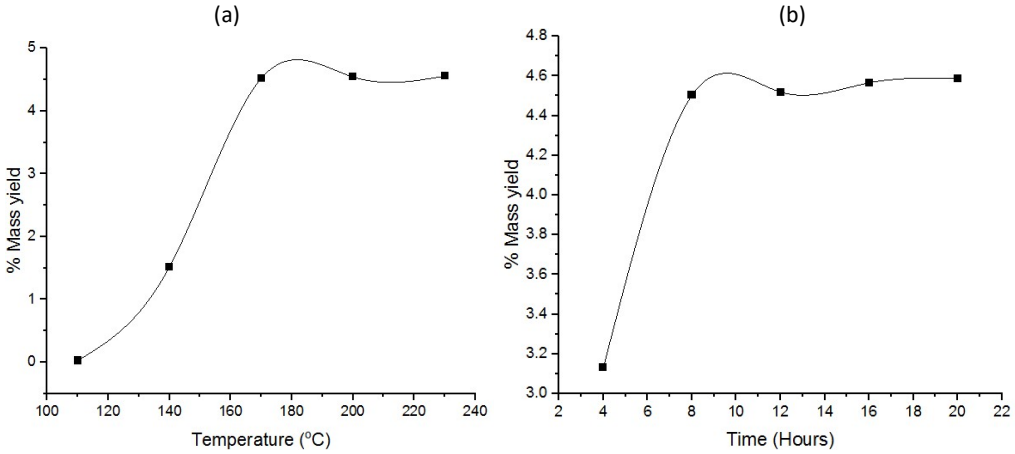

***Fig.1**. %Mass yields at different (a) reaction temperature and (b) reaction time.*

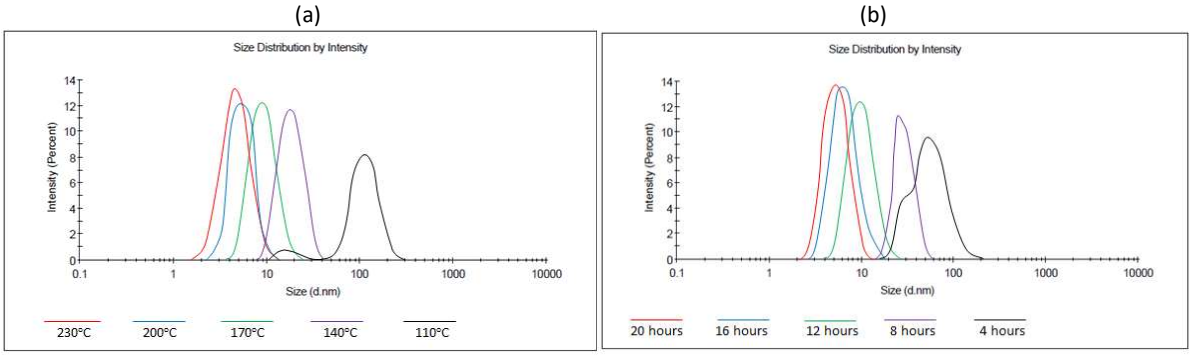

***Fig.2**. DLS results for CQDs at different (a) temperature and (b) time*

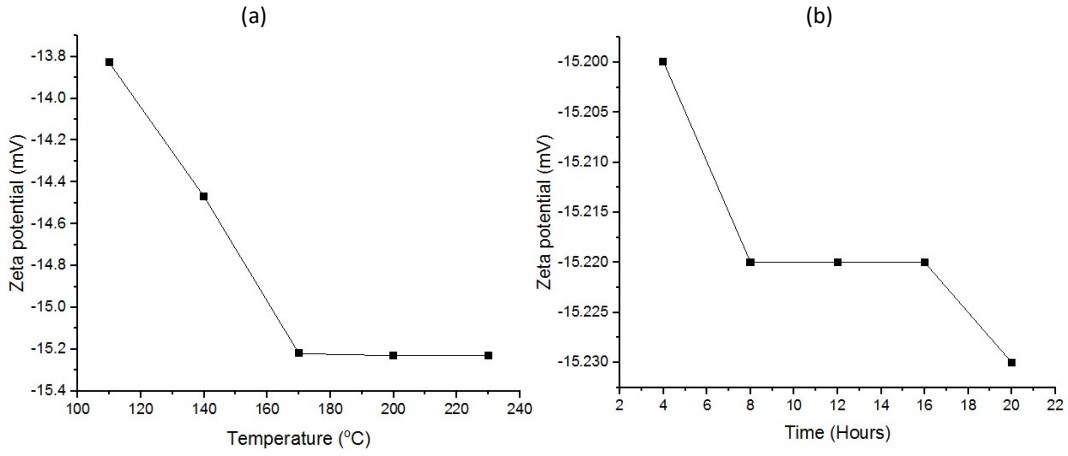

***Fig.3**. Variation of zeta potential with (a) temperature and (b) time*

3.4. Fourier Transform Infra-red (FTIR) Spectroscopy

The different surface functional groups of the CQDs were identified by FTIR (Fig.4). The FTIR spectra of the un-dialyzed CQDs showed the appearance of surface characteristic peaks at 1648, 2973, 1716, 1222, and 1049 cm^{-1} which correspond to –C=C– (aromatic), C–H (aromatic), C=O (ester), C–O–C (epoxy) and C–O functional groups, respectively. The presence of a broad peak at 3612 cm^{-1} could be attributed to hydroxyl C–OH stretching vibrations. After dialysis, better resolved peaks were obtained. The surface characteristic peaks were observed at 1647, 2975, and 1049 cm^{-1} which correspond to –C=C– (aromatic), C–H (aromatic) and C–O functional groups, respectively. The presence of a broad peak at 3645 cm^{-1} could be attributed to hydroxyl C–OH stretching vibrations. The absence of C=O (ester), C–O–C (epoxy) peaks after dialysis could be indicative of the elimination of small biomolecules during the dialysis process.

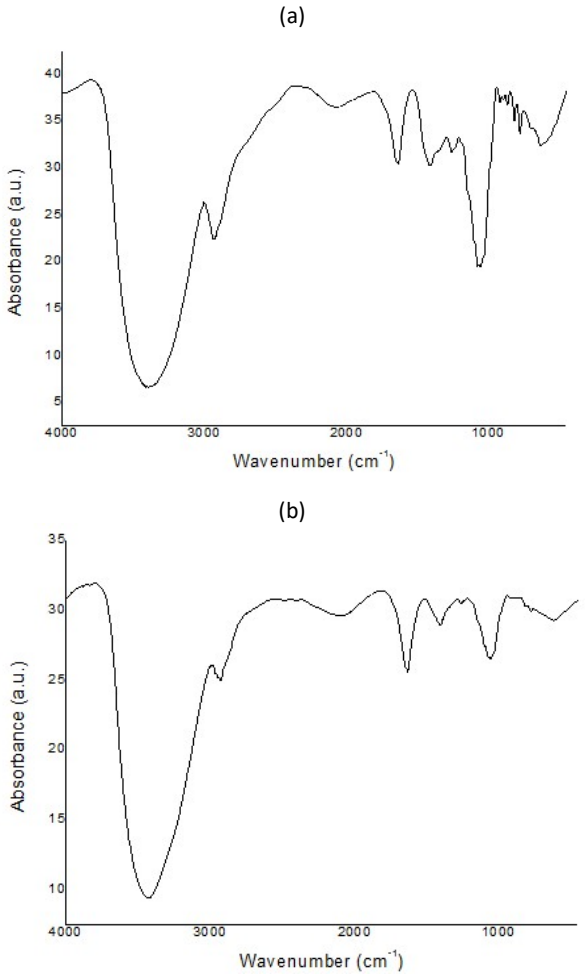

Fig.4*. FTIR spectra of carbon quantum dots (a) before dialysis and (b) after dialysis.*

3.5. Transmission Electron Microscopy (TEM)

The TEM image of the CQDs before dialysis (Fig.5a) reveals a dense packing of carbon nanoparticles with an average particle size of 5 nm. After dialysis (Fig.5b), finely dispersed CQDs were obtained with spherical morphology and an average particle size of 9 nm. The increase in size is likely due to slight agglomeration as a result of the removal of biomolecules. These biomolecules serve as a barrier between adjacent CQDs. Dialysis is still perceived to be of utmost importance because it purifies the CQDs improves the intensity of the green fluorescence observed under UV light.

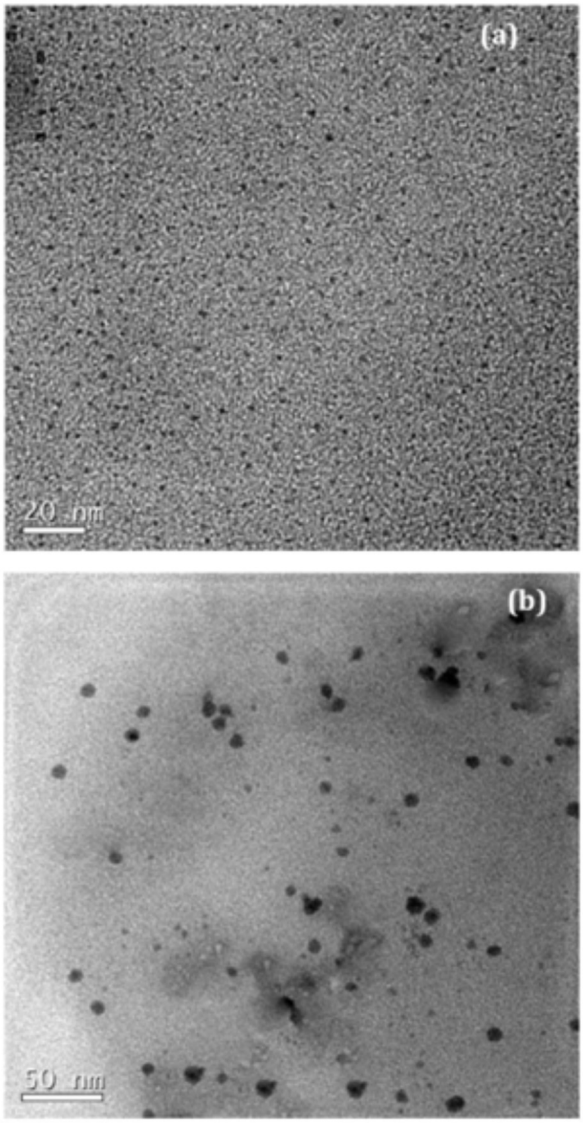

Fig.5*. TEM image for the carbon quantum dots (a) before dialysis and (b) after dialysis.*

3.6. Optical properties of carbon quantum dots

UV/Visible and fluorescence emission spectra were obtained to study the optical properties of the CQDs. For the UV/visible spectrum, the band seen at 273 nm can be attributed to the n-π* and π-π* transitions which are typical of C-O bonds present in carboxyl groups. They can also be attributed to π-π* transitions observed in aromatic C=C bonds. The fluorescence emission spectrum of the CQDs at excitation wavelength of 270 nm is illustrated in Fig.6b. Peaks were observed at 330, 420 and 535 nm. The CQDs exhibited yellow color under visible light but showed green fluorescence under UV light.

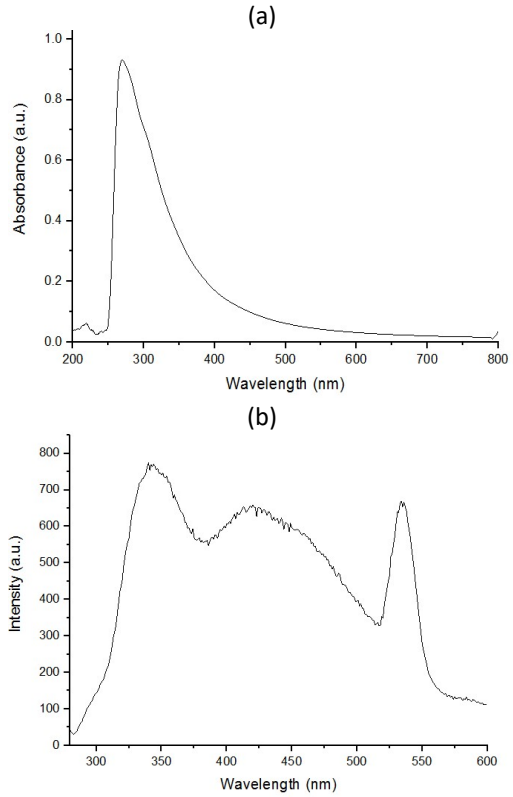

***Fig.6**. (a) UV/visible spectrum of CQDs and (b) Fluorescence emission spectrum of CQDs.*

3.7. Sun protection factor (SPF) determination

The SPF values were obtained to quantitatively evaluate the effectiveness of the UV blocking ability of the CQDs. The absorbance values of CQDs at different concentrations ranging from 0.5 to 10 mg mL^{-1} were recorded between 290 and 320 nm (with an increment of 5 nm). Using the Mansur equation, the SPF values were calculated and presented in the drop line chart below (Fig.7). SPF values generally increased with increasing concentration of CQDs. A sharp increase in the SPF values can be seen between 4 and 8 mg mL^{-1} while a relatively marginal increase in SPF values was observed between 8 and 10 mg mL^{-1}. One can deduct from the results that an aqueous formulation with the CQDs can give an SPF of 35 at a concentration of 10 mg mL^{-1}.

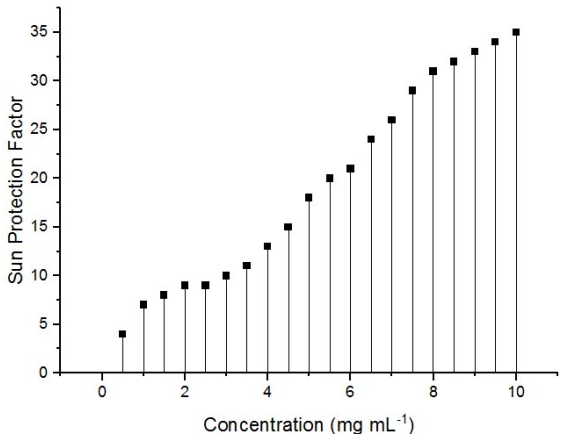

***Fig.7**. Sun Protection Factor (SPF) of CQDs at different concentrations*

4. Conclusion

Carbon quantum dots were successfully synthesized from *Phoenix dactylifera* (date) fruit pulp for potential use as sun protection filters. The percentage mass yields of the CQDs were more significantly affected by the reaction temperature than the reaction time. Average hydrodynamic sizes of the CQDs changed considerably with varied reaction temperatures than with reaction times. However, the reaction temperature was a more consequential factor. Zeta potential values varied broadly with a decrease in zeta potential values as initial reaction temperatures increased. Further increase led to minimal changes in zeta potential. Reaction time had little impact on the zeta potential. Zeta potential values only decreased slightly as reaction times increased. FTIR studies indicated that hydroxyl, carboxyl and carbonyl groups where present in un-dialyzed CQDs. The disappearance of the carbonyl and carboxyl groups after dialysis may be an indication that unwanted biomolecules were eliminated during the dialysis process. TEM images before and after dialysis showed that some nano-sized impurities were eliminated during the dialysis process to produce CQDs with an average particle size of 9 nm. The UV/visible spectrum presented a band with a wavelength of maximum absorption at 273 nm. Fluorescence emission spectrum of CQDs excited at 270 nm showed three bands at 330, 420 and 535 nm. The SPF values of the CQDs generally increased as their concentration increased. A maximum SPF of 35 was obtained at a concentration of 10 mg mL-1. This is comparable with some commercially available UV absorbers and thus, highlights the good UV filtering ability of the CQDs which can be utilized towards the production of sunscreens and other UV filtering applications.

Conflicts of interest

The authors declare that they have no conflict of interest.

Author's statement

O. S. Bankole-Ojo: Conceptualization, Methodology, software, original draft preparation. **F. O. Oyedeji:** Supervision, reviewing and editing.

Acknowledgement

The present research work was funded by CSIR-TWAS Postgraduate fellowship. The authors would like to thank the Director, CSIR-IICT and extend their appreciation to the entire staff and students of Polymers and Functional Materials division, CSIR-IICT, India for their support. Appreciation goes to the authorities of the University of Ibadan, Nigeria for permission granted to execute the research.

References

[1] M.S. Razzaque, The Journal of Steroid Biochemistry and Molecular Biology 175 (2018) 44-48.

[2] L. Marrot, Current Medicinal Chemistry 25(40) (2018) 5469 - 5486.

[3] T.M. Ansary, M.R. Hossain, K. Kamiya, M. Komine, M. Ohtsuki, International Journal of Molecular Sciences 22(8) (2021) 3974.

[4] L.V.M., de Assis, P.N., Tonolli, M.N., Moraes, M.S. Baptista, A.M. de Lauro Castrucci, Journal of Photochemistry and Photobiology C: Photochemistry Reviews 47 (2021) 100403.

[5] P. Li, S., Wang, S. Zhou, Journal of Materials Chemistry C 8 (48) (2020) 17383-17394.

[6] Y.C. Boo, Antioxidants 9(7) (2020) 637.

[7] C. Kang, Y. Huang, H. Yang, X.F. Yan, Z.P. Chen, Nanomaterials 10(11) (2020) 2316.

[8] S. Anwar, H. Ding, M. Xu, X. Hu, Z. Li, J. Wang, H. Bi, ACS Applied Bio Materials 2(6) (2019) 2317-2338.

[9] M. Zulfajri, G. Gedda, C.J. Chang, Y.P. Chang, G.G. Huang, ACS omega 4(13) (2019) 15382-15392.

[10] A.A. Alshatwi, J. Athinarayanan, P.V. Subbarayan, U.S. Patent No. 9,896,342. Washington, DC: U.S. Patent and Trademark Office, 2018.

[11] K., kanthi Gudimella, G., Gedda, P. S., Kumar, B. K., Babu, B., Yamajala, B.V. Rao, P.P. Singh, D. Kumar, A. Sharma, Environmental Research 204 (2022) 111854.

[12] S. Rajamanikandan, M. Biruntha, G. Ramalingam, Journal of Cluster Science 33(3) (2022) 1045-1053.

[13] L. Xiao, H. Sun, Nanoscale Horizons 3(6) (2018) 565-597.

[14] S. Iravani, R.S. Varma, Environmental chemistry letters 18(3) (2020) 703-727.

[15] T.G. Chatzimitakos, A. Kasouni, A. Troganis, I. Leonardos, I. Tzovenis, A. Ntzouvaras, C. Stalikas, C 6(4) (2020) 69.

[16] S. Priyanka, S.R.I. Mary, H.S. Nandini, A.V.M. Kutty, P. Kiranmayee, Asian Journal of Pharmaceutical and Clinical Research 11(2018) 67-71.

[17] A.I. Nicoara, V.L. Ene, B.B. Voicu, M.A. Bucur, I.A. Neacsu, B.S. Vasile, F. Iordache, Nanomaterials 10(3) (2020) 570.